Carbohydrate Polymers 222 (2019) 115025

Contents lists available at ScienceDirect

Carbohydrate Polymers

journal homepage: www.elsevier.com/locate/carbpol

Highly purified fucosylated chondroitin sulfate oligomers with selective intrinsic factor Xase complex inhibition

Lufeng Yan[a,b], Danli Wang[a], Mengshan Zhu[a], Yanlei Yu[b], Fuming Zhang[b], Xingqian Ye[a], Robert J. Linhardt[b,*], Shiguo Chen[a,**]

[a] Zhejiang University, College of Biosystems Engineering and Food Science, Zhejiang Key Laboratory for Agro-Food Processing, Fuli Institute of Food Science, Zhejiang R & D Center for Food Technology and Equipment, Hangzhou 310058, China
[b] Center for Biotechnology & Interdisciplinary Studies and Department of Chemistry & Chemical Biology, Rensselaer Polytechnic Institute, Biotechnology Center 4005, Troy, NY 12180, United States

ARTICLE INFO

Keywords:
Fucosylated chondroitin sulfate oligomers
Partial *N*-deacetylation–deaminative cleavage
Ultrafiltration separation
Anticoagulant and antithrombotic activities
Intrinsic factor Xase complex

ABSTRACT

Fucosylated chondroitin sulfate (FCS) oligosaccharides of specific molecular weight have shown potent anticoagulant activities with selectivity towards intrinsic factor Xase complex. However, the preparation of FCS oligosaccharides by traditional methods requires multiple purification steps consuming large amounts of time and significant resources. The current study focuses on developing a method for the rapid preparation of FCS oligomers from sea cucumber *Pearsonothuria graeffei* having 6–18 saccharide residues. The key steps controlling molecular weight (*M*w) and purity of these FCS oligomers were evaluated. Structural analysis showed the resulting FCS oligomers were primarily L-Fuc3,4diS-α1,3-D-GlcA-β1,3-(D-GalNAc4,6diS-β1,4-[L-Fuc3,4diS-α1,3-]D-GlcA-β1,3-)$_n$D-anTal-ol4,6diS (n = 1~5) accompanied by partial de-fucosylation and/or de-sulfation. *In vitro* and *in vivo* experiments demonstrate that these FCS oligomers selectively inhibit intrinsic factor Xase complex and exhibit remarkable antithrombotic activity without hemorrhagic and hypotension side effects. This method is suitable for large-scale preparation of FCS oligosaccharides as clinical anticoagulants.

1. Introduction

Fucosylated chondroitin sulfate (FCS), found in sea cucumber, is an unusual glycosaminoglycan because of its unique sulfated fucose (Fuc) branches. FCS polysaccharides and their derivatives have showed a variety of bioactivities associated with the control of inflammation (Panagos et al., 2014; Zhao, Zhang et al., 2013), angiogenesis (Tapon-Bretaudiere et al., 2002), hemodialysis (Minamiguchi et al., 2003; Minamiguchi, Kitazato, Sasaki, Nagase, & Kitazato, 1997), cancer metastasis (Borsig et al., 2007), fibrosis (Melo et al., 2010), virus infection (Lian et al., 2013), hyperlipidemia (Wu et al., 2016), atherosclerosis (Igarashi et al., 1997; Tovar & Mourao, 1996), and particularly in coagulation and thrombosis (Chen et al., 2011; Mourao et al., 1996; Zhao et al., 2015). However, the intravenous administration of the FCS polysaccharide can cause a drop in arterial pressure (hypotension), due to the activation of factor XII (FXII) and generation of bradykinin, (Chen et al., 2013; Fonseca et al., 2010; Fonseca, Sucupira, Oliveira, Santos, & Mourao, 2017) and can also result in platelet aggregation (Wu et al., 2015; Yan et al., 2017; Zhao et al., 2015). These side effects severely limit the clinical application of FCS polysaccharides. Fortunately, depolymerized FCS polysaccharide (FCS oligosaccharides) of reduced molecular weight (*M*w) can be prepared, which retain most of FCS bioactivities while avoiding these serious side effects. Depolymerized FCS can selectively inhibit intrinsic factor Xase complex (FXase, factor IXa-VIIIa-Ca^{2+}-phospholipid complex) preventing blood clot formation without increased bleeding risk, suggesting its potential as an anticoagulant and antithrombotic agent (Shang et al., 2018; Zhao et al., 2015).

Currently, the preparation of FCS polysaccharides from the sea cucumber is laborious because following proteolysis it is mixed with fucoidan and pigments from the sea cucumber body wall. Cetylpyridinium chloride (CPC) has generally been used to precipitate the acidic polysaccharides in the protease digestion mixture. The precipitated polysaccharides are then re-dissolved in salt solution and then re-precipitated with alcohol (Chen et al., 2012; Hu et al., 2015). The FCS polysaccharides, thus obtained, often contain residual of toxic CPC and residual pigments. The resulting crude FCS polysaccharides are typically further fractionated by anion-exchange chromatography on a

* Corresponding author.
** Corresponding author at: College of Biosystems Engineering and Food Science, Zhejiang University, Yuhangtang Road 866#, Hangzhou, 310058, China.
E-mail addresses: linhar@rpi.edu (R.J. Linhardt), chenshiguo210@163.com (S. Chen).

https://doi.org/10.1016/j.carbpol.2019.115025
Received 11 May 2019; Received in revised form 7 June 2019; Accepted 24 June 2019
Available online 27 June 2019
0144-8617/ © 2019 Published by Elsevier Ltd.

DEAE-cellulose column using linear salt gradient elution (Chen et al., 2011; Li et al., 2018; Mourao et al., 1996; Wu, Xua, Zhao, Kang, & Ding, 2010; Zancan & Mourao, 2004). Unfortunately, this approach is inappropriate for large-scale preparation as it is both labor-intensive and costly.

After the purification FCS polysaccharides additional steps are then required to prepare FCS oligosaccharides of the appropriate *M*w range. Current FCS depolymerization methods mainly focus on chemical or physical degradation. Acid-catalyzed hydrolysis (Gao, Wu, Li, & Chen, 2014), ^{60}Co irradiation (Wu et al., 2013) and free-radical depolymerization (Wu et al., 2010; Yang et al., 2015) are efficient depolymerization methods but result in random cleavage of glycosidic linkages. Thus, these currently used methods require high purity of FCS polysaccharides to avoid impurities associated with oligosaccharides arising from other polysaccharides. FCS depolymerization by β-elimination (Gao et al., 2015) and partial *N*-deacetylation-deaminative cleavage (Yan et al., 2017; Zhao et al., 2013) shows high selectivity in cleaving FCS polysaccharide chains at certain glycosidic linkages, GalNAc-β1,4-GlcA. Despite this selectively, β-elimination depolymerization is not suitable for large-scale production of FCS oligosaccharides as it involves the use of multi-step reactions controlled with complicated experimental conditions. Partial *N*-deacetylation-deaminative cleavage, by contrast, is more convenient for exclusive preparation of FCS oligosaccharides. Both partial *N*-deacetylation and deaminative cleavage reactions selectively target FCS polysaccharides having little effect on other polysaccharide impurities. The *M*w distribution of the resulting FCS oligosaccharides can be controlled through the degree of FCS deacetylation, which is, in turn, controlled by the hydrazinolysis reaction time (Yan et al., 2017). Thus, crude FCS polysaccharide from sea cucumber are suitable for preparing FCS oligosaccharides of the correct *M*w range by partial *N*-deacetylation–deaminative cleavage followed by simple separation steps.

Sephadex chromatography is useful for oligosaccharides fractionation and purification resulting in a *M*w range of high purity oligosaccharides for structure identification and for bioactivity assessment (Hu et al., 2015; J. Li et al., 2017). However, disadvantages include expensive columns a complicated process and difficulties in scale-up. Membrane separation technology, mainly including ultrafiltration (UF) and nanofiltration (NF), represents a more feasible down-stream strategy for industrial manufacture of such carbohydrate-based products. This technology has a number of advantages including low energy requirements, sustainable processing and relatively easy scale-up (Cano & Palet, 2007; Czermak et al., 2004). The industrial manufacture of carbohydrate oligosaccharides, including arabinoxylo-oligosaccharides, xylo-oligosaccharides and fructo-oligosaccharides prepared through chemical or enzymatic processes have been successfully separated using membrane technology (Pinelo, Jonsson, & Meyer, 2009). For example, oligosaccharides from degree of polymerization 3 to 10 were purified by using UF for separation of larger impurities and using NF for removal of monosaccharides from commercial powder of oligosaccharides from chicory rootstock (Kamada, Nakajima, Nabetani, Saglam, & Iwamoto, 2002).

The present study describes a process including selective depolymerization and membrane separation technology, to efficiently prepare narrowly distributed FCS oligomers. The key processing steps were studied in the quality control of the resulting FCS oligomers. Structural characterization was used to certify high purity product retaining of key structure from FCS polysaccharide. *In vitro* anticoagulant and *in vivo* antithrombotic activity and side effects were evaluated to demonstrate the selective inhibition of the product on intrinsic factor Xase complex and its high safety profile required for potential clinical applications.

2. Materials and methods

2.1. Materials

Dry sea cucumber *Pearsonothuria graeffei* was purchased from a local market in Qingdao (China). The FCS polysaccharide was isolated and purified from the sea cucumber as previously described (Wu et al., 2013). Papain, sodium nitrite, deuterium oxide (D_2O) and chloral hydrate were obtained from Sinopharm Chemical Reagent Co., Ltd. (Shanghai, China). Hydrazine hydrate (containing about 64 wt.% hydrazine in water) and hydrazine sulfate were obtained from Aladdin Reagent (Shanghai, China). Unfractionated heparin (UFH) was obtained from Sigma (St. Louis, MO, USA). LMWH (Enoxaparin, 0.4 mL × 4000 AXaIU) was obtained from Sanofi-Aventis (France). Activated partial thromboplastin time (APTT) assay kits, thrombin time (TT) assay kits, calcium chloride solution (0.02 M) and standard human plasma were obtained from MDC Hemostasis, Germany. Biophen Heparin Anti-FIIa kit, Biophen Heparin Anti-FXa kit and chromogenic assay kit for measuring FVIII: C in concentrates were obtained from Hyphen Biomed (France). Human coagulation FVIII was obtained from China Biologic Products, Inc. (Shandong, China). All other chemicals and reagents were of analytical grade.

2.2. Extraction of crude sea cucumber polysaccharides

Crude sea cucumber polysaccharides were prepared referring to the method reported previously (Li et al., 2016) with modification in process. Briefly, the dried sea cucumber (˜1 kg) was crushed and then was digested with 100 g papain in 20 L of 0.1 M sodium acetate buffer solution (pH 6.0) at 60 °C for 24 h. After boiling for enzyme deactivation, the digestion mixture was centrifuged (4000 rpm, 10 min) and the insoluble impurities were discarded. The clear supernatant was transferred to an ultrafiltration equipment to enrich polysaccharides as showed in Fig. 1(a). The core component ultrafiltration membrane separates large *M*w polysaccharides and small *M*w impurities. The crude polysaccharides were concentrated in storage through reflux liquid while enzymatic peptides and the impurities in the permeate liquid are thrown away. In this process, the concentrated polysaccharides are diluted with pure water for several times until the permeate liquid appeared colorless. However, the final polysaccharides after

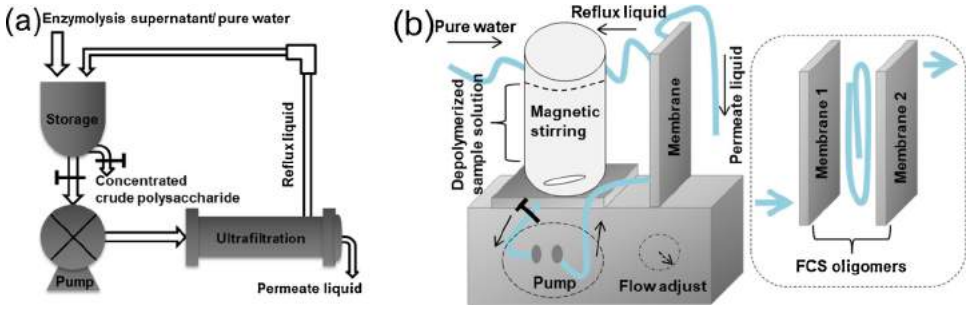

Fig. 1. Membrane separation technology for fast preparation of narrowly distributed FCS oligomers: (a) preparation of crude sea cucumber polysaccharides (b) preparation of FCS oligomers.

lyophilization were unavoidably mixed with dark pigment from the raw sea cucumber due to the molecular viscosity of these polysaccharides.

2.3. Selective depolymerization of FCS

Partial *N*-deacetylation-deaminative cleavage was applied to selectively depolymerize crude FCS polysaccharides as previously described (Yan et al., 2017) with modification. Briefly, the dried crude polysaccharides (200 mg) and 1.50 mL hydrazine hydrate containing 1% hydrazine sulfate are added in a reaction tube. The tube is sealed and incubated at 90 °C for 12 h on a magnetic stirrer at 250 rpm. After the reaction, the solution is added to ethanol (4-times the solution volume). When several drops of saturated sodium chloride are added, precipitates are formed. The precipitate is collected by centrifugation and dissolved in distilled water. This precipitation and dissolution procedure is repeated 4-times to remove the hydrazine and hydrazine sulfate. The resulting solution is dialyzed against flowing tap water for 2 d and distilled water for 1 d with a 3500 Da molecular weight cut-off. After dialysis, the solution is centrifuged in high speed for leaving the dark pigments detached from the glycans and subsequently lyophilized. A series of experiments were performed based on the above representative protocol to analyze the optimal reaction time for the preparation of partial *N*-deacetylated products.

For deaminative cleavage, the nitrous acid reagent was prepared by mixture of 0.5 M H_2SO_4 and 5.5 M $NaNO_2$ at volume ratio of 3:5. Next, 1 mL ice-cold 40 mg/mL *N*-deacetylated products solution was added to 2 mL pre-cooling nitrous acid reagent in a reaction tube. The reaction was performed for 10 min in an ice bath, and the excess nitrous acid was neutralized by addition of 1.5 mL 0.5 M NaOH. Immediately, 150 μL 300 mg/mL $NaBH_4$ (dissolved in 0.05 M NaOH) was added and reduced at 50 °C for 2 h. The sample was then dialyzed with a 500 Da molecular weight cut-off as described above.

2.4. Preparation of FCS oligomers

Depolymerized sample solution was transferred to another membrane separation equipment for producing FCS oligomers as showed in Fig. 1(b). The solid arrows indicate the direction of liquid flow in the pipelines. Membrane 1 is used for retaining large *M*w polysaccharides while the membrane 2 was used for removing small *M*w oligosaccharides. After these two separations, the resulting solution containing FCS oligomers was obtained and lyophilized.

2.5. Molecular weight measurement

Molecular weight (*M*w) measurement of samples was determined by high performance gel permeation chromatography (HPGPC) and glucan standards were used to determine the *M*w of the samples. The crude polysaccharides and partial *N*-deacetylated products were performed on a Waters Ultrahydrogel 500 column (3.9 × 300 mm) (Milford, MA, USA) eluted by 0.2 M NaCl aqueous solution at the flow rate 0.5 mL/min monitored with a refractive index detector. The *M*w distribution of depolymerized products and FCS oligomers were analyzed using a Superdex Peptide 10/300 G L column (10 × 300 mm) eluted by 0.2 M NaCl at the flow rate 0.4 mL/min monitored with a refractive index detector.

2.6. Relative viscosity and color difference

The solution (1 mg/mL) viscosity of crude polysaccharides and different *N*-deacetylation time samples were measured using an Ubbelohde viscometer (Zhejiang Jiaojiang Glass Instrument Factory, China). Briefly, 10 mL of sample solution was measured its effluent time (t^*) in the ubbelohde viscometer (inner diameter 0.4-0.5 mm, viscosity constant 0.003604 mm^2/s^2) at a constant temperature of 20 ± 0.5 °C. The relative viscosity (Η) was calculated as follows: $\Eta = t^*/t_0$, where t_0 is the effluent time of pure water.

The solution (1 mg/mL) color of samples were measured with a colorimeter (ColorFlex EZ, HunterLab) (Rojas-Grau, Sobrino-Lopez, Tapia, & Martin-Belloso, 2006). Color was recorded using a CIE $L^* a^* b^*$ color space, where L^* indicates lightness, a^* indicates chromaticity on a green (−) to red (+) axis, and b^* chromaticity on a blue (−) to yellow (+) axis. The color difference ($^{\triangle}E$) was calculated as follows: $^{\triangle}E = [(L^* - L_0)^2 + (a^* - a_0)^2 + (b^* - b_0)^2]^{1/2}$, where L_0, a_0 and b_0 are the color values of pure water. All determinations were conducted in triplicate and the results were reported as mean with standard deviation.

2.7. Nuclear magnetic resonance spectroscopy and hydrophilic interaction liquid chromatography-Fourier transform mass spectrometry analysis

For nuclear magnetic resonance (NMR) spectroscopy, samples (30 mg) were dissolved in 500 μL of D_2O (99.9%) and lyophilized three times to substitute the exchangeable protons, and then dissolved in 500 μL D_2O, and finally transferred to NMR microtubes. In addition, ^1H, ^{13}C, ^1H-^1H COSY and $^1H/^{13}C$ HSQC NMR experiments were performed on a Hudson-Bruker SB 600 MHz Spectrometer (Madison, WI, USA) at room temperature.

FCS oligomers product was dissolved in 50% acetonitrile as 1 mg/mL for online hydrophilic interaction chromatography (HILIC) Fourier transform mass spectrometry (FTMS) analysis, which was performed on an Agilent 1290 LC UPLC system (Agilent Technologies, Wilmington, DE, USA) equipped with a LTQ ORBITRAP XL mass spectrometer (Thermo, SCIENTIFIC, USA). FCS oligomers were separated by a Luna HILIC column (150 × 2.00 mm, 3 μm, Phenomenex) at 25 °C. The mobile phase was a mixture of 5 mM NH_4OAc/98% acetonitrile (solvent A) and 5 mM NH_4OAc/H_2O (solvent B) at a flow rate of 150 μL/min. The gradient was programmed as 92% A in the beginning, linearly changed to 60% A in 58 min. The analysis was performed in the negative ion mode using a capillary temperature of 275 °C. The spray voltage was 4.2 kV and nitrogen dry gas flowed at 40 L/min. Data acquisition and analysis were performed using Xcalibur 2.0 software.

2.8. Anticoagulant activity

The activated partial thromboplastin time (APTT) and thrombin time (TT) assays were determined with a coagulometer (RAC-120, China) using APTT and TT reagents and standard human plasma as previously described (Gao et al., 2012). The results were expressed as international IU/mg using a parallel standard curve based on the International Heparin Standard (212 IU/mg).

Anti-thrombin (anti-FIIa) and anti-factor Xa (anti-FXa) activities in the presence of antithrombin (AT) and samples, and inhibition of intrinsic factor Xase complex in the presence of samples were carried out in a 96-well micro-titerplate as described (Wu et al., 2015). The absorbance change rate was proportional to the FIIa and FXa activity remaining in the incubation mixtures. The experimental results were expressed as the percent of control (n = 3). EC_{50} values were obtained by fitting the data to a noncompetitive inhibition model for the samples according to Sheehan and Walke (Sheehan & Walke, 2005).

2.9. Venous thrombosis

Antithrombotic activity in rats was assessed using rabbit brain thromboplastin as the thrombogenic stimulus (Zhao et al., 2015). Male Sprague Dawley rats (body weight 250–300 g) were randomly segregated into 4 groups of 8 animals each. The control group, LMWH group and two doses of FCS oligomers were administered dorsally and *subcutaneously* with 1 mL/kg body weight of 0.86% NaCl, 4 mg/kg body weight of LMWH, and 5 and 10 mg/kg body weight of FCS oligomers, respectively. After 60 min, rats were anesthetised with an intramuscular injection of 100 mg/kg body weight of ketamine and 16 mg/kg body

weight of xylazine, the inferior *vena cava* and its branches were isolated, and the branch of inferior *vena cava* under the left renal vein was ligated. A volume of 1 mL/kg body weight of 2% tissue thromboplastin was injected from the femoral vein. After 20 s, stasis was established by ligating the edge of the left renal vein. After a 20 min stasis, the cavity was then reopened, the ligated segment was opened longitudinally, and the thrombus formed was removed, rinsed, dried for 24 h at 50 °C, and then weighed. The results were reported as mean with standard deviation.

2.10. Bleeding effect

Blood loss was determined by measuring the hemoglobin present in the water using a spectrophotometric method (Fonseca et al., 2017; Zhao et al., 2015). Male Kunming mice (body weight 18–22 g) were randomly segregated into 3 groups of 6 animals each. The control group, LMWH group and FCS oligomers group were administered dorsally and *subcutaneously* 5 mL/kg body weight of 0.86% NaCl, 40 mg/kg body weight of LMWH, and 120 mg/kg body weight of FCS oligomers, respectively. After 60 min, the tails of the mice were cut 5 mm from the tip and immersed in 40 mL of distilled water for 90 min at 37 °C with stirring. The volume of blood was determined from a standard curve based on absorbance at 540 nm.

2.11. Arterial blood pressure and heart rate

Male Sprague Dawley rats (body weight 250–300 g) were randomly segregated into FCS polysaccharide and FCS oligomers groups of 5 animals each to measure the arterial pressure and heart rate. Rats were anesthetised with a combination of xylazine and ketamine as described earlier, and a P10 catheter was inserted into both the right femoral vein and artery. The arterial catheter was connected to a pressure transducer (MP150, BIOPAC Systems Inc.) coupled to an acquisition system (AcqKnowledge, BIOPAC Systems Inc.) After a 10-min adaptation period, the rats were administered 10 mg/kg of FCS polysaccharide or FCS oligomers as an aqueous solution, and then the systolic, diastolic, mean arterial blood pressures and the heart rate were continuously monitored. At the end of the observation period, the animals were euthanized using KCl (10 mg/kg).

3. Results and discussion

3.1. Preparation of narrowly distributed FCS oligomers

The *M*w properties and appearance of samples at different preparation stages were investigated to evaluate feasibility of a new process for FCS oligomer production (Fig. 2). The HPGPC profiles of crude polysaccharides shown in Fig. 2(a) indicate that ultrafiltration with suitable membrane can be used to enrich FCS and fucoidan from sea cucumber proteolytic liquid in a cost effective and pollution-free manner replacing traditional ethanol or CPC-based precipitation (Chen et al., 2012; Hu et al., 2015). However, the high viscosity of these crude polysaccharides prevented the removal of the dark pigment impurity despite multiple washing steps resulting in a highly colored lyophilized sample.

Partial *N*-deacetylation of FCS by treatment with hydrazine, also dramatically decreased the *M*w of both FCS and fucoidan as shown in Fig. 2(b). We speculate that this *M*w change was caused by the β-eliminative cleavage under these alkaline conditions, since the β-eliminative cleavage of FCS and heparan sulfate in hydrazine has been previously reported (Guo & Conrad, 1989; Yan et al., 2017). In addition, the dark pigment was eliminated in this step as shown by the white appearance of lyophilized sample. We attribute this de-colorization to the complete dissolution of polymer chains under hot alkaline conditions as well as the partial *N*-deacetylation of FCS. A more expensive and complicated anion-exchange step also resulted in the same de-coloring effect.

Since the deaminative cleavage is specific at the *N*-deacetylated position of FCS polysaccharide (Zhao et al., 2015), FCS oligomers having trisaccharide-repeating units were generated while fucoidan maintained its high *M*w as shown in Fig. 2(c). Thus, there was major difference in *M*w of FCS oligomers and fucoidan polysaccharides making it easy to separate and purify the FCS oligomers using a membrane with a suitable pore diameter. The resulting HPGPC profiles for the FCS oligomers (6–18 mers), shown in Fig. 2(d), indicate that the membrane 1 successfully retained fucoidan and large *M*w FCS (> 18-mer) while the membrane 2 easily removed low *M*w FCS oligomers (< 6-mer). Polyacrylamide gel electrophoretograms (PAGE) analysis of the FCS oligomers product (Supplementary Fig. S1) also showed that membrane cutting succeeded in getting 6–18 mers with little other fragments.

3.2. Study of key process steps for product quality control

N-deacetylation time could be easily adjusted to control partial *N*-deacetylation and deaminative cleavage of purified FCS polysaccharide (Yan et al., 2017). Thus, the effects of *N*-deacetylation time on relative viscosity of *N*-deacetylated products, the color difference of *N*-deacetylated products, the *M*w distribution of *N*-deacetylated products and the *M*w distribution of depolymerized products were investigated to optimize the *N*-deacetylation time of the crude polysaccharide preparation (Fig. 3). The results indicate that hydrazine treatment for 4 h was sufficient to reduce the relative viscosity of polysaccharides solution and disaggregate chains eliminating the dark pigment as shown in Fig. 3(a) & (b). Longer hydrazine treatments time had negligible influence on relative viscosity and de-coloration of the polysaccharide solution, which suggests that a 4 h hydrazine treatment was adequate for the crude polysaccharide. Extension of reaction time decreased the *M*w of FCS component in crude polysaccharides when compared to that of the purified FCS polysaccharide as shown in Fig. 3(c). The degree of depolymerization FCS rose (Fig. 3(d)) as the *N*-deacetylation degree of FCS increased in the partial *N*-deacetylation–deaminative cleavage of purified FCS (Yan et al., 2017). FCS fragments of 3–12.0 kDa have been shown to be safe and effective selective inhibitors of intrinsic tenase complex (Yan et al., 2017; Zhao et al., 2015), and moderate depolymerization resulting from a 10–12 h *N*-deacetylation time afforded appropriately sized FCS oligomers (6–18 mers). The similar distribution of oligomers from 12 h *N*-deacetylation of crude polysaccharide mixture and purified FCS polysaccharide observed indicate that the presence of fucoidan and dark pigments had no impact on this selective FCS depolymerization and generated no obvious impurities in the resulting FCS oligomers product.

3.3. NMR spectral analysis of FCS oligomers

The FCS oligomers product (shown in Fig. 2(d)) was analyzed by NMR spectroscopy to characterize its structure and compare with FCS polysaccharide as shown in Fig. 4. The FCS oligomers product was clearly similar to the FCS polysaccharide precursor based on their ^{1}H and ^{13}C NMR spectra (Fig. 4(a)–(d)). The signals at 1.9–2.2 ppm, 1.2–1.5 ppm and ~24.0 ppm, ~17.6 ppm in the ^{1}H and ^{13}C NMR spectra of FCS polysaccharide and FCS oligomers were assigned to the methyl (CH_3) signals of GalNAc and Fuc, respectively. The H-1 signal at ~5.34 ppm and C-1 signal at ~100.7 ppm were assigned to the 3,4-*O*-disulfated Fuc branch (Fuc3,4S) and occupied the majority of the Fuc branches on both polysaccharide and oligosaccharide chains (Chen et al., 2013). These sulfated Fuc branches were stable during the entire preparation process. There were some obvious structural differences between FCS polysaccharide and FCS oligomers. In the 1D spectra, anTal-ol residue was found at the new reducing end of the FCS oligomers through the observation of the H-4 signal at ~5.06 ppm and C-1 signal at ~62.6 ppm. The signals for the GlcA and Fuc residues at the

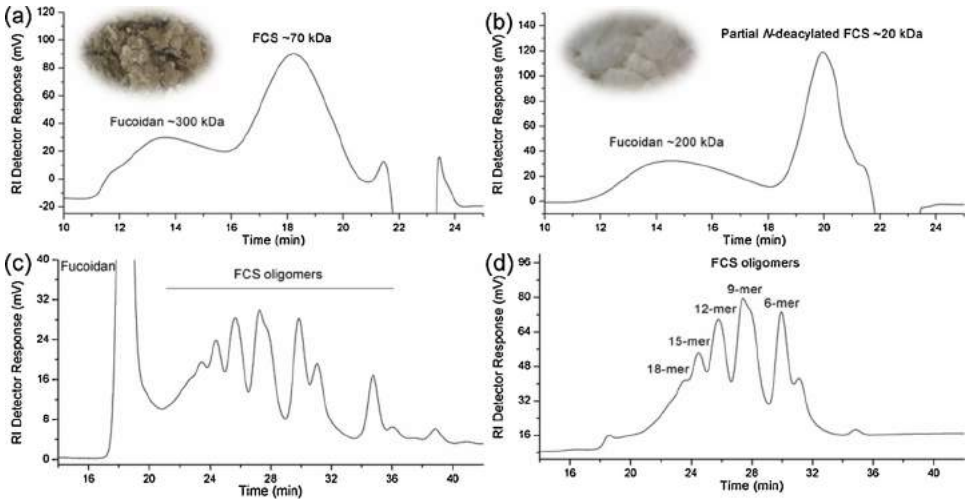

Fig. 2. HPGPC profiles of products on different preparation stages: (a) Crude polysaccharides; (b) Partial *N*-deacetylated product; (c) Depolymerized product; (d) FCS oligomers. Appearance of lyophilized sample (a) and (b) were showed in the corresponding figure, respectively.

terminus of oligosaccharide chains were obviously shifted from those of FCS polysaccharide. For example, in the ^{1}H NMR spectrum, new signals appeared at ˜5.13 ppm and ˜1.24 ppm, could be assigned to H-1 and H-6 of Fuc3,4S residues at the terminus of the FCS oligomers. Similarly, in the ^{13}C NMR spectrum, new signals appearing at ˜102.1 ppm and ˜17.5 ppm could be assigned to C-1 and C-6 of these Fuc3,4S residues, respectively.

The results of 2D NMR spectra, including correlation spectroscopy (COSY) (Fig. 4(e)) and heteronuclear single quantum coherence (HSQC) (Fig. 4(f)) also allowed the assignment of some new signals at the new terminus of FCS oligomers. The H-5 (4.49 ppm) of new terminal Fuc3,4S residues and the H-4 (3.68 ppm) of new terminal GlcA residue were shifted more than any other proton in the same saccharide ring because of the change in their chemical environment resulting from the cleavage of glycosidic linkage between GalNAc and GlcA. In addition, the H-1 (4.54 ppm) and C-1 (102.6 ppm) in the middle GlcA residue were obviously shifted due to the adjacent newly formed anTal-ol residue. There were obvious shifts in the signals for GalNAc, since the terminal GalNAc had been converted to an anTal-ol residue through deamination. For example, the proton signals at 3.80, 4.14 ppm and the carbon signals at 62.6, 82.4 ppm were assigned to the H-1, H-2 and C-1, C-2 of anTal-ol, respectively. The ^{1}H and ^{13}C NMR signals of FCS oligomers product with its FCS polysaccharide precursor (cited from reference (Chen et al., 2013)) are assigned in Supplementary Table S1. In general, FCS oligomers product prepared by this new method was highly pure and had the same structure as observed in product prepared by partial *N*-deacetylation–deaminative depolymerization of pure FCS polysaccharide (Wu et al., 2013, 2015; Yan et al., 2017).

3.4. HILIC-FTMS analysis of FCS oligomers product

The structures of the FCS oligomers were also determined by HILIC-FTMS. The total ion chromatogram (TIC) revealed several peaks, which were mainly separated according to their *M*w differences (Supplementary Fig. S2). The components within the retention time of each peak were selected for MS analysis. In each MS analysis of an ion chromatogram peak, the ion peaks of high relative abundance were selected for structural identification (Supplementary Fig. S3).

Eighteen main fragments of FCS oligomers were identified as shown in Table 1 and most of these contained the previously described

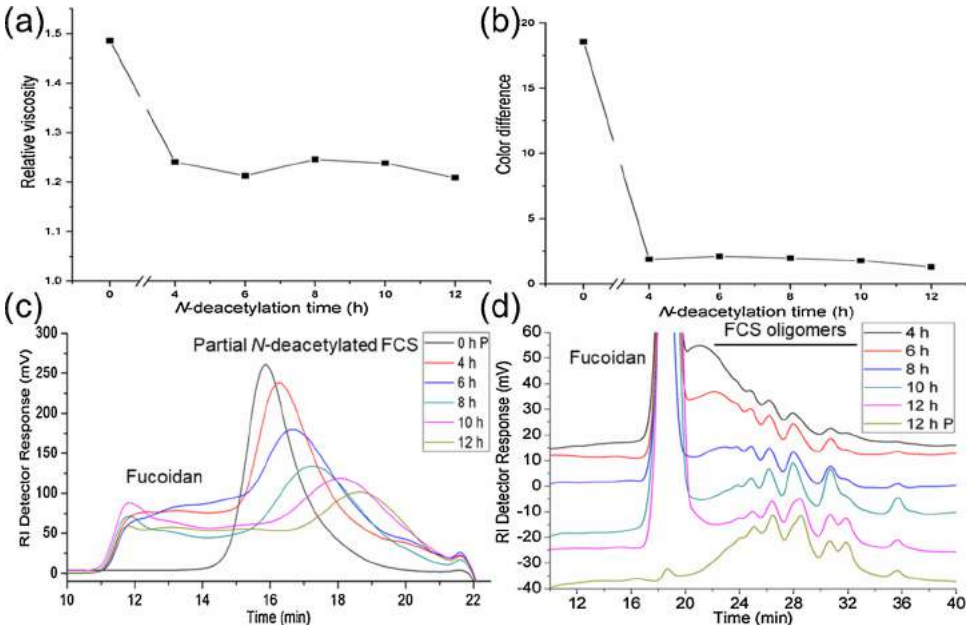

Fig. 3. Characterization of products from different *N*-deacetylation time: (a) Relative viscosity (ɳ) of partial *N*-deacetylated product solutions; (b) Color difference (△E) of partial *N*-deacetylated product solutions; (c) HPGPC profiles of partial *N*-deacetylated products; (d) HPGPC profiles of depolymerized products. "0 h P" and "12 h P" indicate purified FCS polysaccharide and its depolymerized product, respectively.

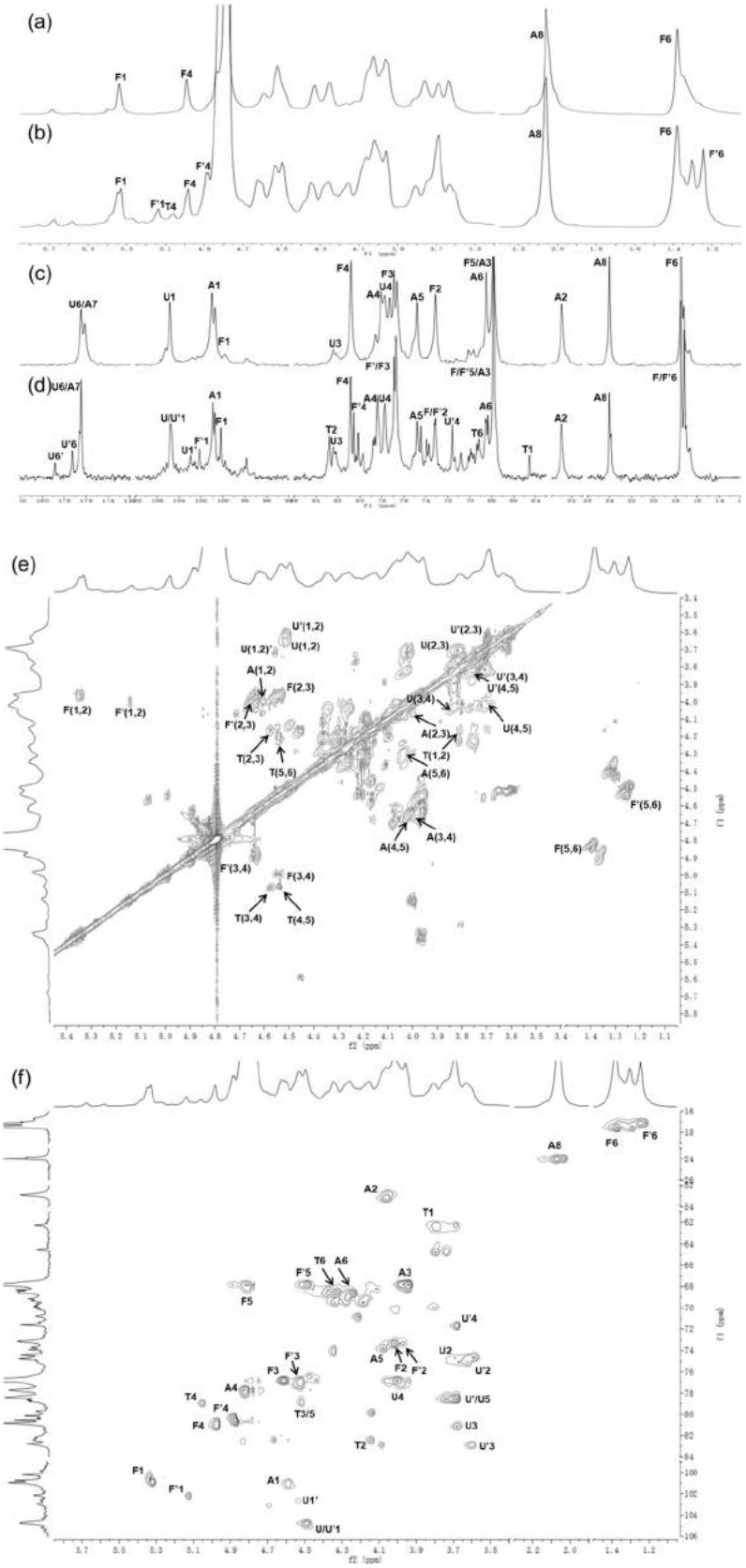

Fig. 4. Structural analysis of FCS oligomers product: ^{1}H (a) and ^{13}C (c) NMR spectra of FCS polysaccharide; ^{1}H (b), ^{13}C (d), ^{1}H-^{1}H COSY (e) and $^{1}H/^{13}C$ HSQC (f) NMR spectra of FCS oligomers product. Labels U, F and A represent GlcA, Fuc and GalNAc residues, in the middle of the chains, respectively. Labels U' and F' represent GlcA and Fuc residues at new terminus of the chains, respectively, and label T represents an anTal-ol residue at the new reducing end.

Table 1
Composition identification of major peaks from total ion chromatography of FCS oligomers product.

m/z	Charge	*M*w	Composition	Fragment
522.67	3	1568.01	[2GlcA•GalNAc•2Fuc•anTal-ol•7S-3 H]$^{3-}$	6-mer
549.32	3	1647.96	[2GlcA•GalNAc•2Fuc•anTal-ol•8S-3 H]$^{3-}$	
−741.02	3	2223.06	[3GlcA•2GalNAc•2Fuc•anTal-ol•10S + 2NH_3-3 H]$^{3-}$	8-mer
414.99	6	2489.94	[3GlcA•2GalNAc•3Fuc•anTal-ol•12S-6 H]$^{6-}$	−9-mer
848.01	3	2544.03	[3GlcA•2GalNAc•3Fuc•anTal-ol•12S + 3NH_3-3 H]$^{3-}$	
−859.36	3	2578.08	[3GlcA•2GalNAc•3Fuc•anTal-ol•12S + 5NH_3-3 H]$^{3-}$	
−775.77	4	3103.08	[4GlcA•3GalNAc•3Fuc•anTal-ol•14S + 4NH_3-4 H]$^{4-}$	−11-mer
1045.72	3	3137.16	[4GlcA•3GalNAc•3Fuc•anTal-ol•14S + 6NH_3-3 H]$^{3-}$	
−465.14	7	3255.98	[4GlcA•3GalNAc•4Fuc•anTal-ol•15S-7 H]$^{7-}$	−12-mer
476.56	7	3335.92	[4GlcA•3GalNAc•4Fuc•anTal-ol•16S-7 H]$^{7-}$	
−860.02	4	3440.08	[4GlcA•3GalNAc•4Fuc•anTal-ol•16S + 6NH_3-4 H]$^{4-}$	
−868.78	4	3475.12	[4GlcA•3GalNAc•4Fuc•anTal-ol•16S + 8NH_3-4 H]$^{4-}$	
−1004.04	4	4016.16	[5GlcA•4GalNAc•4Fuc•anTal-ol•18S + 8NH_3-4 H]$^{4-}$	−14-mer
512.49	8	4099.92	[5GlcA•4GalNAc•5Fuc•anTal-ol•19S-8 H]$^{8-}$	−15-mer
522.49	8	4179.92	[5GlcA•4GalNAc•5Fuc•anTal-ol•20S-8 H]$^{8-}$	
−1088.55	4	4354.20	[5GlcA•4GalNAc•5Fuc•anTal-ol•20S + 10NH_3-4 H]$^{4-}$	
−1241.08	4	4964.32	[6GlcA•5GalNAc•6Fuc•anTal-ol•23S + NH_3-4 H]$^{4-}$	−18-mer
1317.32	4	5269.28	[6GlcA•5GalNAc•6Fuc•anTal-ol•24S + 14NH_3-4 H]$^{4-}$	

"S" represents a sulfur trioxide group.

trisaccharide-repeating units. For example, ions of *m/z* 549.32 with 3 negative charges exactly matched the composition of [2GlcA•GalNAc•2Fuc•anTal-ol•8S-3 H]$^{3-}$, which is expected for a FCS 6-mer afforded through partial *N*-deacetylation–deaminative cleavage (Yan et al., 2017; Zhao et al., 2015). In addition, a small number of desulfated oligomers were also detected, such as ions of *m/z* 1241.08 with 4 negative charges, which exactly matched the composition of [6GlcA•5GalNAc•6Fuc•anTal-ol•23S + NH_3-4 H]$^{4-}$ as a 18-mer with a loss of SO_3. Partial non-fucosylated FCS oligomers were also observed in MS analysis. For example, ions of *m/z* 775.77 with 4 negative charges matches an 11-mer of composition [4GlcA•3GalNAc•3Fuc•anTal-ol•14S + 4NH_3-4 H]$^{4-}$. Furthermore, the distribution of main fragments in the MS analysis was similar to that observed by HPGPC, with 12-mer representing the major component. Based on previous descriptions of the FCS polysaccharides (Chen et al., 2013) and our NMR analysis of FCS oligomers, their structure could be summarized as L-Fuc3,4diS-α1,3-D-GlcA-β1,3-(D-GalNAc4,6diS-β1,4-[L-Fuc3,4diS-α1,3-]D-GlcA-β1,3-)$_n$D-anTal-ol4,6diS (n = 1~5) with some partial lack of fucosylation and/or desulfation.

3.5. Anticoagulant properties of FCS oligomers product

FCS oligomers product show a narrow *M*w distribution mainly 6–18 mers and retain the key structure of the FCS polysaccharide precursor, including Fuc branch and sulfation. According to previous reports (Wu et al., 2015; Yan et al., 2017; Zhao et al., 2015), these FCS oligomers should show potent anticoagulant activity with selective inhibition on intrinsic factor Xase complex. Thus, the anticoagulant properties, including APTT, TT, anti-FIIa/AT, anti-FXa/AT and anti-FXase, of FCS oligomers together with FCS polysaccharide, UFH and LMWH were investigated (Table 2). The concentration required for doubling APTT of FCS oligomers was ~5-fold greater than the FCS polysaccharide and the concentration required for doubling TT of FCS oligomers was much higher than that of FCS polysaccharide. TT was much more affected by a decreased *M*w than APTT and this was consistent with the activity of FCS from the same sea cucumber with depolymerized ^{60}Co irradiation (Wu et al., 2013). APTT measures interference with the intrinsic coagulation cascade and the TT measures the last step of the coagulation cascade, thrombin-mediated fibrin formation (Lin et al., 2007). This suggests that FCS oligomers become much more active in the intrinsic pathway.

The anticoagulant activities of anti-FIIa/AT, anti-FXa/AT and anti-FXase were investigated and compared with FCS polysaccharide, UFH and LMWH to better understand the anticoagulant mechanism of the FCS oligomers. All these activities were decreased in the FCS oligomers compared to the FCS polysaccharide. However, AT-dependent anti-FXa activity of FCS oligomers (4.15 IU/mg) was over 4-times the AT-dependent anti-FIIa activity of FCS oligomers (< 1.00 IU/mg) although the FCS polysaccharide had weaker intensity in AT-dependent anti-FXa (18.2 IU/mg) than anti-FIIa activities (20.8 IU/mg). The weak ability of the FCS oligomers to inactivate FIIa by AT was likely due to loss of allosteric activation effect on AT binding to FIIa (Xiao et al., 2016), and this is distinctly important in reducing side effects such as bleeding (Kitazato, Kitazato, Sasaki, Minamiguchi, & Nagase, 2003). In addition, the FCS oligomers retained potent anti-FXase (65.7 IU/mg) activity, which was much more than their anti-FIIa/AT and anti-FXa/AT activities. These results are consistent with previous reports on depolymerized FCS fragments from the sea cucumber *Isostichopus badionotus* (Yan

Table 2
Anticoagulant properties of FCS oligomers product.

Compd.	*M*w size[a]	APTT		TT		anti-FIIa/AT		anti-FXa/AT		anti-FXase	
		μg/mL[b]	IU/mg[c]	μg/mL[b]	IU/mg[c]	μg/mL[d]	IU/mg[c]	μg/mL[d]	IU/mg[c]	μg/mL[d]	IU/mg[c]
FCS polysaccharide	~73.0 kDa	20.9	122	9.84	190	5.08	20.8	5.49	18.2	0.33	234
FCS oligomers	6–18 mers	112	22.7	> 128	< 14.6	> 1000	< 1.00	24.0	4.15	1.17	65.7
UFH	~18.0 kDa	12.0	212	8.81	212	0.50	212	0.47	212	0.36	212
LMWH	~4.50 kDa	36.5	69.6	33.1	56.4	1.53	69.2	0.88	113	1.39	55.4

[a] The *M*w size of FCS polysaccharide, UFH and LMWH were determined by HPGPC. The *M*w size of FCS oligomers was expressed as trisaccharide-repeating units according to Fig. 2(d).
[b] The concentration required to double the APTT/TT of human plasma (APTT/TT doubling).
[c] The activity is expressed as international IU/mg using a parallel standard curve based on the International Heparin Standard (212 IU/mg).
[d] IC_{50} value, the concentration required to inhibit 50% of protease activity.

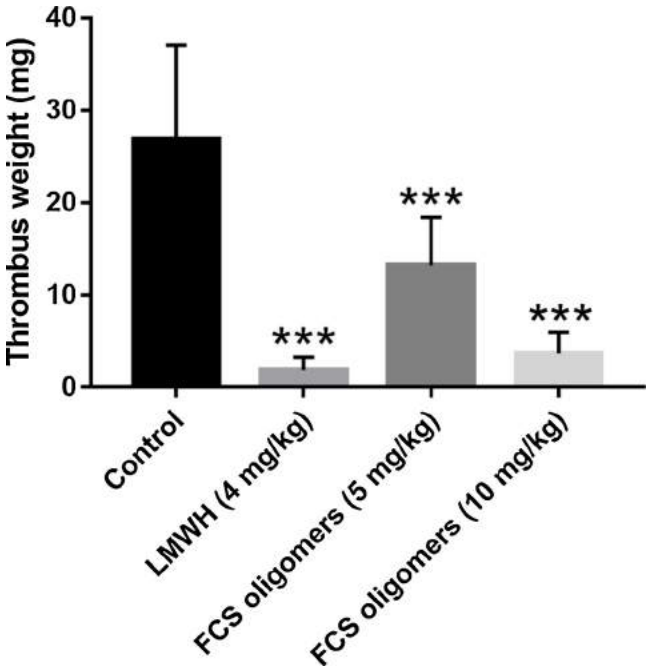

Fig. 5. Venous antithrombotic activity of FCS oligomers *in vivo*. The results were expressed as thrombus weight (mean ± SD, n = 8, $^{**}P < 0.01$, $^{***}P < 0.001$ *vs*. control).

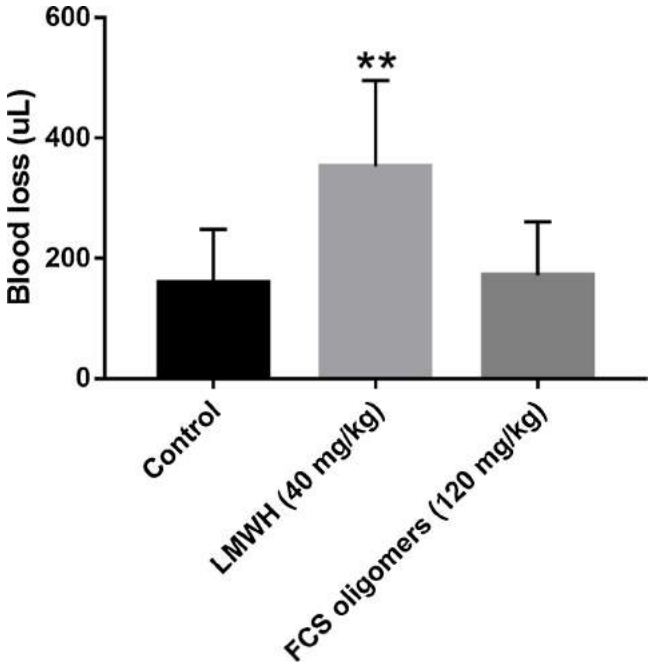

Fig. 6. Bleeding effect of FCS oligomers *in vivo*. The results were expressed as microliters of blood loss (mean ± SD, n = 6, $^{**}P < 0.01$ *vs*. control).

et al., 2017). In conclusion, FCS oligomers exhibit powerful anti-FXase activity with weak anti-FXa/AT activity and negligible anti-FIIa/AT activity. Although FCS oligomers showed reduced anticoagulant properties compared to FCS polysaccharide, their anticoagulant mechanism became simplified as selective inhibitors of the intrinsic coagulation pathway, the final and rate-limiting enzyme complex, the inhibition of which does not risk serious bleeding.

3.6. Antithrombotic activity of FCS oligomers product in vivo

Anticoagulant data suggested that FCS oligomers exhibit strong *in vitro* anticoagulant activities by selectively inhibiting human intrinsic tenase. Therefore, we further determined the antithrombotic activity of FCS oligomers compared with LMWH *in vivo* as shown in Fig. 5. In the venous thrombosis model, FCS oligomers exhibited strong inhibition of venous thrombus formation with thrombosis inhibition rates of 50.7% and 86.4% at doses of 5 and 10 mg/kg, respectively. The thrombosis inhibition of LMWH was 93.1% at 4 mg/kg. In previous studies, it has been shown that the inhibition of thrombus formation of LMWH is mainly related to its anti-FXa/AT activity (Mackman, 2008). In this study, based on the previous anticoagulant properties assays (Table 2), the antithrombotic property of FCS oligomers is attributed to selective inhibition of the intrinsic tenase.

3.7. Side effects of FCS oligomers product in vivo

Previous *in vitro* studies have shown that depolymerized FCS with *M*w < 12 kDa has negligible side effects, such as the activation of human FXII and the induction of platelet aggregation (Wu et al., 2015; Yan et al., 2017). We determined its bleeding and hypotension risk *in vivo* to further verify the safety of these FCS oligomers. The effect of FCS oligomers on blood loss in mouse model is shown in Fig. 6. Compared with the blood loss of the normal control group, negative control LMWH obviously increased blood loss at a dose of 40 mg/kg ($P <$ 0.01). FCS oligomers had no obvious effects even at a three-fold higher dose of 120 mg/kg ($P >$ 0.05). This suggests that FCS oligomers are safer than LMWH for clinical application due to their targeting at the

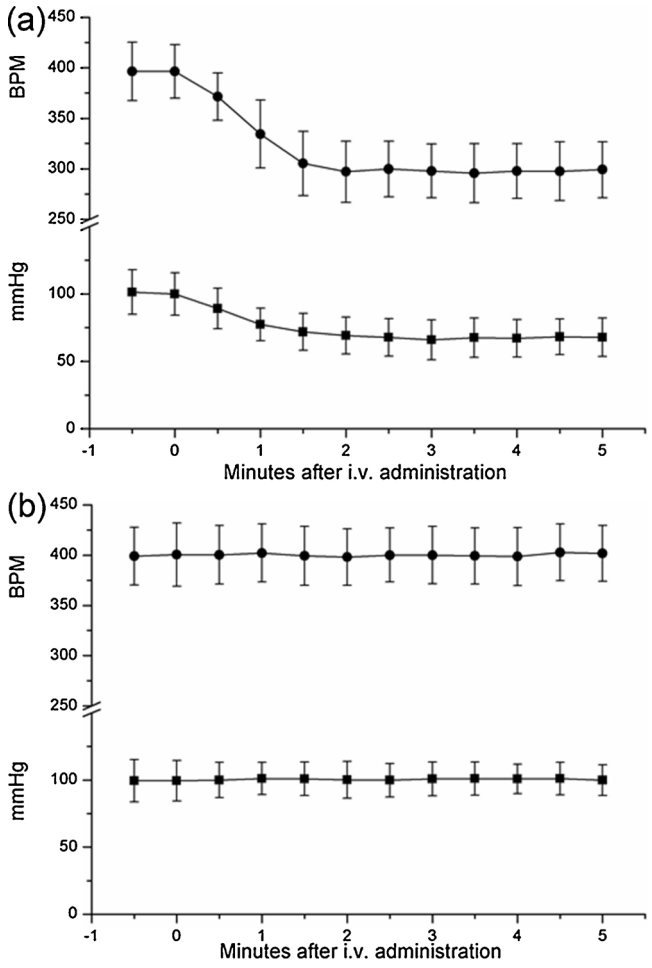

Fig. 7. Effects of FCS polysaccharide (a) and FCS oligomers (b) administered by intravascular injection on rat heart rate (closed circles, BPM) and arterial blood pressure (closed squares, as mmHg).

intrinsic tenase rather than the AT-dependent anti-FXa mechanism.

The evaluation of FCS oligomers in rat hypotension model is shown in Fig. 7. Administration of FCS polysaccharide immediately generated adverse effect of hypotension and a reduced heart rate, which were caused by the activation of FXII (Chen et al., 2013; J.H. Li et al., 2017) and the following generation of bradykinin (Fonseca et al., 2010). In addition, hypotension and reduced heart rate could not resolve in a short time, because FCS polysaccharide kept circulating in the blood without enzyme degradation (Mourao et al., 1996). In contrast, FCS oligomers did not result in hypotension and reduced heart rate, which can be attributed to their failure to activate FXII, due to their low *M*w (Yan et al., 2017).

4. Conclusion

In the present study, we used a rapid method for the preparation of narrowly distributed FCS oligomers. These oligomers were produced from FCS polysaccharide from raw sea cucumber *Pearsonothuria graeffei* and were mainly in range of 2–6 trisaccharide-repeating units (6–18 mers). The method used to produce these FCS oligomers involved a membrane separation for preparation of crude polysaccharides, followed by a selective depolymerization of crude FCS polysaccharide by partial *N*-deacetylation–deaminative cleavage and another membrane separation for preparation of FCS oligomers. After process optimization, we confirmed the appropriate conditions in key reaction step to afford highly bioactive FCS oligomers. Structural analysis by NMR and HILIC-FTMS showed the high purity FCS oligomers maintained the Fuc branches and sulfation pattern consistent with FCS polysaccharide precursor. *In vitro* and *in vivo* investigation of anticoagulation, antithrombosis and side effects indicated that this FCS oligomers showed potent antithrombotic activity based on anticoagulant effect of selective inhibition on intrinsic factor Xase complex without risk of bleeding and hypotension. Thus, this new preparation method is suitable for production of targeting *M*w narrowly distributed FCS oligomers from sea cucumbers for potential clinical anticoagulation application.

Acknowledgements

The authors are grateful to the National Natural Science Foundation of China (31871815) and 2018 Zhejiang University Academic Award for Outstanding Doctoral Candidates. Lufeng Yan is supported by the China Scholarship Council for two-year study at Rensselaer Polytechnic Institute.

Appendix A. Supplementary data

Supplementary material related to this article can be found, in the online version, at doi:https://doi.org/10.1016/j.carbpol.2019.115025.

References

Borsig, L., Wang, L. C., Cavalcante, M. C. M., Cardilo-Reis, L., Ferreira, P. L., Mourao, P. A. S., et al. (2007). Selectin blocking activity of a fucosylated chondroitin sulfate glycosaminoglycan from sea cucumber - Effect on tumor metastasis and neutrophil recruitment. *Journal Of Biological Chemistry, 282*(20), 14984–14991.

Cano, A., & Palet, C. (2007). Xylooligosaccharide recovery from agricultural biomass waste treatment with enzymatic polymeric membranes and characterization of products with MALDI-TOF-MS. *Journal Of Membrane Science, 291*(1–2), 96–105.

Chen, S., Hu, Y., Ye, X., Li, G., Yu, G., Xue, C., et al. (2012). Sequence determination and anticoagulant and antithrombotic activities of a novel sulfated fucan isolated from the sea cucumber Isostichopus badionotus. *Biochimica et Biophysica Acta, 1820*(7), 989–1000.

Chen, S., Li, G., Wu, N., Guo, X., Liao, N., Ye, X., et al. (2013). Sulfation pattern of the fucose branch is important for the anticoagulant and antithrombotic activities of fucosylated chondroitin sulfates. *Biochimica et Biophysica Acta, 1830*(4), 3054–3066.

Chen, S. G., Xue, C. H., Yin, L. A., Tang, Q. J., Yu, G. L., & Chai, W. G. (2011). Comparison of structures and anticoagulant activities of fucosylated chondroitin sulfates from different sea cucumbers. *Carbohydrate Polymers, 83*(2), 688–696.

Czermak, P., Ebrahimi, M., Grau, K., Netz, S., Sawatzki, G., & Pfromm, P. H. (2004). Membrane-assisted enzymatic production of galactosyl-oligosaccharides from lactose in a continuous process. *Journal of Membrane Science, 232*(1–2), 85–91.

Fonseca, R. J. C., Oliveira, S. N. M. C. G., Pomin, V. H., Mecawi, A. S., Araujo, I. G., & Mourao, P. A. S. (2010). Effects of oversulfated and fucosylated chondroitin sulfates on coagulation challenges for the study of anticoagulant polysaccharides. *Thrombosis and Haemostasis, 103*(5), 994–1004.

Fonseca, R. J. C., Sucupira, I. D., Oliveira, S. N. M. C. G., Santos, G. R. C., & Mourao, P. A. S. (2017). Improved anticoagulant effect of fucosylated chondroitin sulfate orally administered as gastro-resistant tablets. *Thrombosis and Haemostasis, 117*(4), 662–670.

Gao, N., Lu, F., Xiao, C., Yang, L., Chen, J., Zhou, K., et al. (2015). Beta-Eliminative depolymerization of the fucosylated chondroitin sulfate and anticoagulant activities of resulting fragments. *Carbohydrate Polymers, 127*, 427–437.

Gao, N., Wu, M., Liu, S., Lian, W., Li, Z., & Zhao, J. (2012). Preparation and characterization of O-acylated fucosylated chondroitin sulfate from sea cucumber. *Marine Drugs, 10*(8), 1647–1661.

Gao, R. C., Wu, N., Li, Y., & Chen, S. G. (2014). Structures and anticoagulant activities of the partially mild acidic hydrolysis products of the fucosylated chondroitin sulfate from sea cucumber Pearsonothuria graeffei. *Journal of Carbohydrate Chemistry, 33*(9), 471–488.

Guo, Y., & Conrad, H. E. (1989). The disaccharide composition of heparins and heparan sulfates. *Analytical Biochemistry, 176*(1), 96–104.

Hu, Y. Q., Li, S., Li, J. H., Ye, X. Q., Ding, T., Liu, D. H., et al. (2015). Identification of a highly sulfated fucoidan from sea cucumber Pearsonothuria graeffei with well-repeated tetrasaccharides units. *Carbohydrate Polymers, 134*, 808–816.

Igarashi, M., Takeda, Y., Mori, S., Takahashi, K., Fuse, T., Yamamura, M., et al. (1997). Depolymerized holothurian glycosaminoglycan (DHG) prevents neointimal formation in balloon-injured rat carotid artery. *Atherosclerosis, 129*(1), 27–31.

Kamada, T., Nakajima, M., Nabetani, H., Saglam, N., & Iwamoto, S. (2002). Availability of membrane technology for purifying and concentrating oligosaccharides. *European Food Research and Technology, 214*(5), 435–440.

Kitazato, K., Kitazato, K. T., Sasaki, E., Minamiguchi, K., & Nagase, H. (2003). Prolonged bleeding time induced by anticoagulant glycosaminoglycans in dogs is associated with the inhibition of thrombin-induced platelet aggregation. *Thrombosis Research, 112*(1–2), 83–91.

Li, J., Li, S., Yan, L., Ding, T., Linhardt, R. J., Yu, Y., et al. (2017). Fucosylated chondroitin sulfate oligosaccharides exert anticoagulant activity by targeting at intrinsic tenase complex with low FXII activation: Importance of sulfation pattern and molecular size. *European Journal of Medicinal Chemistry, 139*, 191–200.

Li, J. H., Li, S., Yan, L. F., Ding, T., Linhardt, R. J., Yu, Y. L., et al. (2017). Fucosylated chondroitin sulfate oligosaccharides exert anticoagulant activity by targeting at intrinsic tenase complex with low FXII activation: Importance of sulfation pattern and molecular size. *European Journal of Medicinal Chemistry, 139*, 191–200.

Li, J. H., Li, S., Zhi, Z. J., Yan, L. F., Ye, X. Q., Ding, T., et al. (2016). Depolymerization of fucosylated chondroitin sulfate with a modified fenton-system and anticoagulant activity of the resulting fragments. *Marine Drugs, 14*(9).

Li, Q. Y., Cai, C., Chang, Y. G., Zhang, F. M., Linhardt, R. J., Xue, C. H., et al. (2018). A novel structural fucosylated chondroitin sulfate from Holothuria mexicana and its effects on growth factors binding and anticoagulation. *Carbohydrate Polymers, 181*, 1160–1168.

Lian, W., Wu, M. Y., Huang, N., Gao, N., Xiao, C., Li, Z., et al. (2013). Anti-HIV-1 activity and structure-activity-relationship study of a fucosylated glycosaminoglycan from an echinoderm by targeting the conserved CD4 induced epitope. *Biochimica Et Biophysica Acta-General Subjects, 1830*(10), 4681–4691.

Lin, C. Z., Guan, H. S., Li, H. H., Yu, G. L., Gu, C. X., & Li, G. Q. (2007). The influence of molecular mass of sulfated propylene glycol ester of low-molecular-weight alginate on anticoagulant activities. *European Polymer Journal, 43*(7), 3009–3015.

Mackman, N. (2008). Triggers, targets and treatments for thrombosis. *Nature, 451*(7181), 914–918.

Melo, N. M., Belmiro, C. L., Goncalves, R. G., Takiya, C. M., Leite, M., Pavao, M. S. G., et al. (2010). Fucosylated chondroitin sulfate attenuates renal fibrosis in animals submitted to unilateral ureteral obstruction: a P-selectin-mediated event? *American Journal of Physiology-Renal Physiology, 299*(6), F1299–F1307.

Minamiguchi, K., Kitazato, K. T., Nagase, H., Sasaki, E., Ohwada, K., & Kitazato, K. (2003). Depolymerized holothurian glycosaminoglycan (DHG), a novel alternative anticoagulant for hemodialysis, is safe and effective in a dog renal failure model. *Kidney International, 63*(4), 1548–1555.

Minamiguchi, K., Kitazato, K. T., Sasaki, E., Nagase, H., & Kitazato, K. (1997). The anticoagulant and hemorrhagic effects of DHG, a new depolymerized holothurian glycosaminoglycan, on experimental hemodialysis in dogs. *Thrombosis and Haemostasis, 77*(6), 1148–1153.

Mourao, P. A. S., Pereira, M. S., Pavao, M. S. G., Mulloy, B., Tollefsen, D. M., Mowinckel, M. C., et al. (1996). Structure and anticoagulant activity of a fucosylated chondroitin sulfate from echinoderm - Sulfated fucose branches on the polysaccharide account for its high anticoagulant action. *Journal Of Biological Chemistry, 271*(39), 23973–23984.

Panagos, C. G., Thomson, D. S., Moss, C., Hughes, A. D., Kelly, M. S., Liu, Y., et al. (2014). Fucosylated chondroitin sulfates from the body wall of the sea cucumber Holothuria forskali conformation, selectin binding, and biological activity. *Journal Of Biological Chemistry, 289*(41), 28284–28298.

Pinelo, M., Jonsson, G., & Meyer, A. S. (2009). Membrane technology for purification of enzymatically produced oligosaccharides: Molecular and operational features affecting performance. *Separation And Purification Technology, 70*(1), 1–11.

Rojas-Grau, M. A., Sobrino-Lopez, A., Tapia, M. S., & Martin-Belloso, O. (2006). Browning inhibition in fresh-cut' fuji' apple slices by natural antibrowning agents. *Journal Of Food Science, 71*(1), S59–S65.

Shang, F. N., Gao, N., Yin, R. H., Lin, L., Xiao, C., Zhou, L. T., et al. (2018). Precise structures of fucosylated glycosaminoglycan and its oligosaccharides as novel

intrinsic factor Xase inhibitors. *European Journal of Medicinal Chemistry, 148*, 423–435.
Sheehan, J. P., & Walke, E. N. (2005). Depolymerized holothurian glycosaminoglycan and heparin inhibit the intrinsic tenase complex by a common antithrombin-independent mechanism. *Blood, 106*(11), 296a 296a.
Tapon-Bretaudiere, J., Chabut, D., Zierer, M., Matou, S., Helley, D., Bros, A., et al. (2002). A fucosylated chondroitin sulfate from echinoderm modulates in vitro fibroblast growth factor 2-dependent angiogenesis. *Molecular Cancer Research, 1*(2), 96–102.
Tovar, A. M. F., & Mourao, P. A. S. (1996). High affinity of a fucosylated chondroitin sulfate for plasma low density lipoprotein. *Atherosclerosis, 126*(2), 185–195.
Wu, M., Wen, D., Gao, N., Xiao, C., Yang, L., Xu, L., et al. (2015). Anticoagulant and antithrombotic evaluation of native fucosylated chondroitin sulfates and their derivatives as selective inhibitors of intrinsic factor Xase. *European Journal of Medicinal Chemistry, 92*, 257–269.
Wu, M. Y., Xua, S. M., Zhao, J. H., Kang, H., & Ding, H. (2010). Physicochemical characteristics and anticoagulant activities of low molecular weight fractions by free-radical depolymerization of a fucosylated chondroitin sulphate from sea cucumber Thelenata ananas. *Food Chemistry, 122*(3), 716–723.
Wu, N., Ye, X. Q., Guo, X., Liao, N. B., Yin, X. Z., Hu, Y. Q., et al. (2013). Depolymerization of fucosylated chondroitin sulfate from sea cucumber, Pearsonothuria graeffei, via Co-60 irradiation. *Carbohydrate Polymers, 93*(2), 604–614.
Wu, N. A., Zhang, Y., Ye, X. Q., Hu, Y. Q., Ding, T., & Chen, S. G. (2016). Sulfation pattern of fucose branches affects the anti-hyperlipidemic activities of fucosylated chondroitin sulfate. *Carbohydrate Polymers, 147*, 1–7.
Xiao, C., Lian, W., Zhou, L., Gao, N., Xu, L., Chen, J., et al. (2016). Interactions between depolymerized fucosylated glycosaminoglycan and coagulation proteases or inhibitors. *Thrombosis Research, 146*, 59–68.
Yan, L. F., Li, J. H., Wang, D. L., Ding, T., Hu, Y. Q., Ye, X. Q., et al. (2017). Molecular size is important for the safety and selective inhibition of intrinsic factor Xase for fucosylated chondroitin sulfate. *Carbohydrate Polymers, 178*, 180–189.
Yang, J., Wang, Y., Jiang, T., Lv, L., Zhang, B., & Lv, Z. (2015). Depolymerized glycosaminoglycan and its anticoagulant activities from sea cucumber Apostichopus japonicus. *International Journal of Biological Macromolecules, 72*, 699–705.
Zancan, P., & Mourao, P. A. S. (2004). Venous and arterial thrombosis in rat models: dissociation of the antithrombotic effects of glycosaminoglycans. *Blood Coagulation & Fibrinolysis, 15*(1), 45–54.
Zhao, L., Wu, M., Xiao, C., Yang, L., Zhou, L., Gao, N., et al. (2015). Discovery of an intrinsic tenase complex inhibitor: Pure nonasaccharide from fucosylated glycosaminoglycan. *Proceedings of the National Academy of Sciences of the United States of America, 112*(27), 8284–8289.
Zhao, L. Y., Lai, S. S., Huang, R., Wu, M. Y., Gao, N., Xu, L., et al. (2013). Structure and anticoagulant activity of fucosylated glycosaminoglycan degraded by deaminative cleavage. *Carbohydrate Polymers, 98*(2), 1514–1523.
Zhao, Y., Zhang, D. H., Wang, S., Tao, L., Wang, A. Y., Chen, W. X., et al. (2013). Holothurian glycosaminoglycan inhibits metastasis and thrombosis via targeting of nuclear factor-kappa B/tissue factor/factor Xa pathway in melanoma B16F10 cells. *PloS One, 8*(2).